Raft-like osmium- and ruthenium-antimony carbonyl clusters

Li, Ying-Zhou; Leong, Weng Kee

2015

Li, Y.-Z., & Leong, W. K. (2015). Raft-like osmium- and ruthenium-antimony carbonyl clusters. Journal of Organometallic Chemistry, 812, 217-225.

https://hdl.handle.net/10356/79334

https://doi.org/10.1016/j.jorganchem.2015.06.007

Raft-like Osmium- and Ruthenium-Antimony Carbonyl Clusters

Ying-Zhou Li, and Weng Kee Leong*

Division of Chemistry & Biological Chemistry, Nanyang Technological University, 21 Nanyang Link, Singapore, 637371

Abstract: The higher nuclearity raft-like cluster $Os_6(CO)_{20}(\mu\text{-}SbPh_2)_2$, **5-Os**, was isolated from the base hydrolysis of $Os_3(CO)_{11}(SbPh_2Cl)$, **1-Os**. The ruthenium analogue, *viz*., $Ru_6(CO)_{20}(\mu\text{-}SbPh_2)_2$, **5-Ru**, was obtained from the reduction of $Ru_3(CO)_{12}$, **7-Ru**, with the benzophenone ketyl radical followed by treatment with $SbPh_2Cl$. These clusters undergo facile ligand substitution reactions with two-electron donors to afford the mono- and disubstituted derivatives $M_6(CO)_{20-n}(\mu\text{-}SbPh_2)_2(L)_n$, (M = Ru or Os; n = 1 (**8**) or 2 (**9**); L = PMe_3 (**a**), PPh_3 (**b**), or ^{t}BuNC (**c**)).

Keywords: Raft-like clusters; Higher nuclearity carbonyl clusters; Osmium; Ruthenium; Antimony

Introduction

A great number of high nuclearity homo- or heterometallic Group 8 metal carbonyl clusters have been reported but most of them adopt three-dimensional, polyhedral configurations, such as, the (distorted) octahedron (for hexanuclear clusters) and more complex polyhedra (for heptanuclear and higher nuclearity clusters). Two-dimensional planar or quasi-planar (raft-like), higher nuclearity clusters containing six or more metal atoms are relatively rare. They usually show distinct physical and reactivity properties [1] including some which show interesting magnetic properties [2].

* Corresponding author. Tel: +65 6592 7577. E-mail: chmlwk@ntu.edu.sg

To our knowledge, the only high-nuclearity homometallic osmium clusters with almost planar metal cores are $Os_6(CO)_{21-n}(NCCH_3)_n$, ($n$ =0, 1 or 2), and their several phosphine, acetylene, or 2-aldrithiol substitution derivatives [3]; ruthenium analogues are unknown. Heterometallic examples containing osmium or ruthenium include a number of clusters of the general formulae $M_3(CO)_{12}[M'(L)]_n$ (M = Os or Ru; M' = Pd or Pt; L = P^tBu_3 or NHC; n = 1-3) [1c,4]. The metal cores in the latter group of clusters are rather distorted from planarity and have been referred to simply as "two-dimensional" clusters. Examples containing a main group metal or metalloid include several with Ge or Sn, obtained via the addition of germylene [5] or Ph_3MH (M = Ge or Sn) [6], to $M_3(CO)_{12}$ (M = Os or Ru), or via the pyrolysis of low-nuclearity osmium [7], or ruthenium [8], clusters containing Ge ligands; these cluster tend to be planar.

We have been investigating synthetic routes to osmium-antimony clusters [9], and serendipitously uncovered the almost planar, raft-like, higher nuclearity clusters $M_6(CO)_{20}(\mu\text{-}SbPh_2)_2$, **5-M** (where M = Os or Ru). Our study into their formation and their substitution chemistry is reported here.

Results and discussion

Oxidative addition of the Sb-Cl bond in $SbPh_2Cl$ to $Os_3(CO)_{11}(NCCH_3)$ occurs via the substitution product $Os_3(CO)_{11}(SbPh_2Cl)$, **1-Os**, to eventually form $Os_3(CO)_{11}(\mu\text{-}SbPh_2)(Cl)$, **2-Os** [10]. During our investigations into the conversion of **1-Os** to **2-Os**, we found that the addition of H_2O and Na_2CO_3 afforded the previously reported clusters **2-Os**, **3-Os** and **4-Os**, and two other clusters, one of which is the new raft-like, higher nuclearity cluster $Os_6(CO)_{20}(\mu\text{-}SbPh_2)_2$, **5-Os** (Scheme 1).

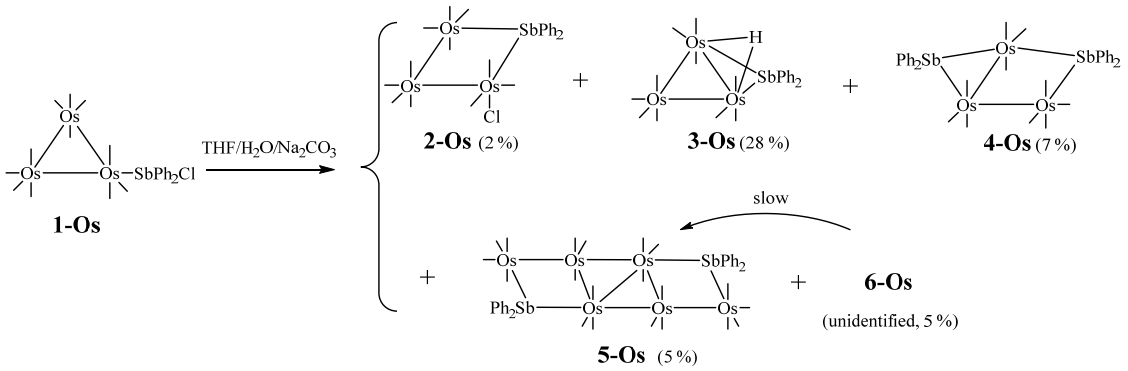

Scheme 1. Base hydrolysis of $Os_3(CO)_{11}(SbPh_2Cl)$, **1-Os**.

Cluster **5-Os** is stable under ambient conditions over several months and has been fully characterized, including by an X-ray crystallographic analysis. An ORTEP plot depicting its structure is given in Fig. 1. The other unidentified product **6-Os** was found to gradually convert to **5-Os**, especially in a polar solvent such as MeOH, as was evident by monitoring the conversion through ^{1}H NMR spectroscopy (see supplementary data Fig. S3). Its HRMS spectrum showed a similar pattern to that of **5-Os** (see supplementary data Fig. S22 (a) and (b)), suggesting that it was probably an isomer.

We have also carried out some studies into the reaction pathway in the hope of increasing the yield of **5-Os**. As mentioned above, we have shown earlier that **2-Os** resulted from oxidative addition of the Sb-Cl bond in **1-Os** [20]. Cluster **4-Os** was presumably the result of reaction of **3-Os** with $SbPh_2Cl$, generated from **1-Os** via ligand dissociation or decomposition [11]. On monitoring the base hydrolysis of **1-Os** (in *d*-THF) by ^{1}H NMR spectroscopy, four metal hydride resonances (δ = -8.72, -8.27, -8.97 and -9.19 ppm) were observed after 8 h (see supplementary data Fig. S5).

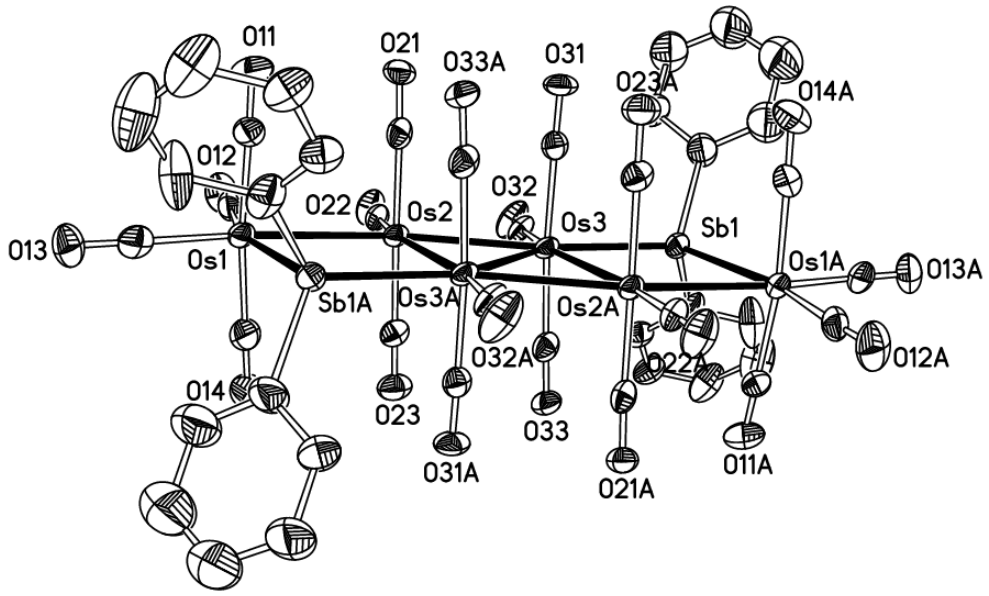

Fig. 1. ORTEP plot of the molecular structure of **5-Os** (one of two asymmetrical molecules) with thermal ellipsoids at the 50% probability level. Organic hydrogen atoms have been omitted for clarity.

Treatment of **2-Os** under the same reaction conditions gave **3-Os** as the sole separable product in a much higher yield (*ca*. 75%), albeit with a much longer reaction time (*ca*. 72h) for completion [12]; no **5-Os** was observed. This suggested that the formation of **5-Os** (and **6-Os**) followed a different reaction pathway from that for clusters **2-Os** to **4-Os**. The ^{1}H NMR spectrum of this latter reaction showed only two metal hydride resonances (δ = -8.27 and -8.97 ppm) after 24 h (see supplementary data Fig. S4). These hydride species probably resulted from a Hieber reaction under the basic conditions employed. Based on these observations, the proposed reaction pathways to all the products are as given in Scheme 2.

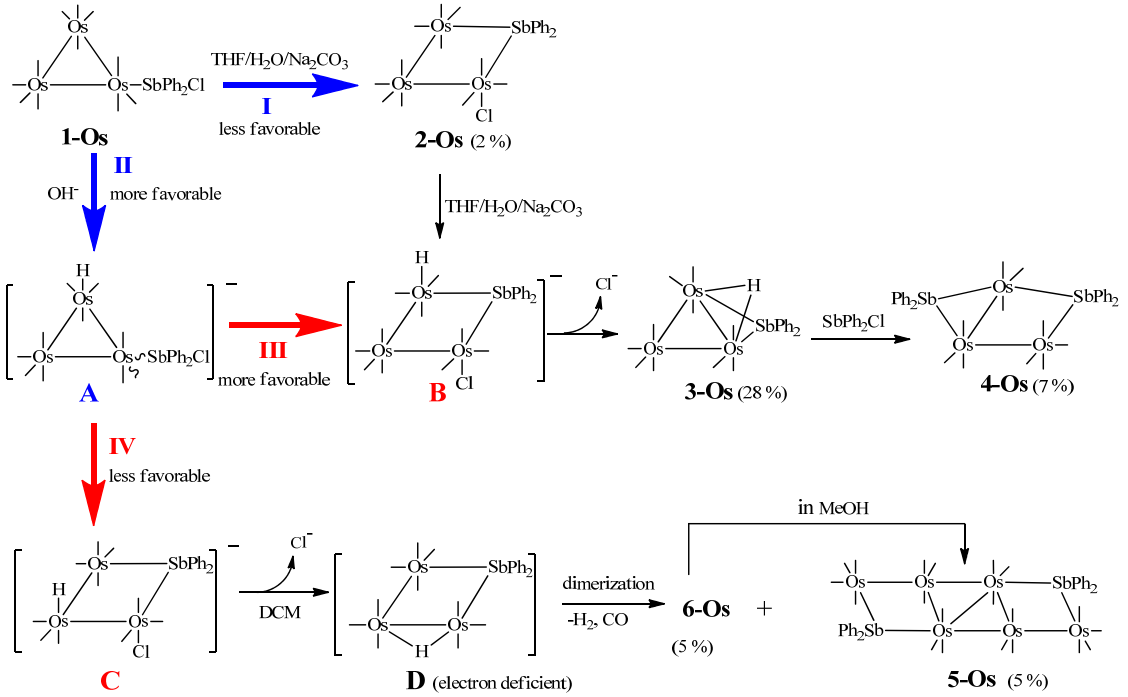

Scheme 2. Proposed reaction pathways for the base hydrolysis of **1-Os**.

It is suggested that **3-Os** is formed via two competitive pathways (**I** and **II**), through **2-Os** or the intermediate **A**. Presumably, there are two possible isomers of **A**, corresponding to the different relative orientation of the $SbPh_2Cl$ and the terminal H ligands; oxidative addition of the Sb-Cl bond across an Os-Os bond in one leads to **B** and further on to **3-Os** via a chloride elimination, while the other leads to **C** and further on to an electron-deficient cluster **D** via a similar pathway. This latter quickly converts to **5-Os** and **6-Os** through further elimination of H_2 and CO.

The metal hydride resonances at δ = -8.27 and -8.97 ppm may thus be assigned to **B** (and its isomer with the opposite orientation of H) and the other two resonances observed in the reaction of **1-Os** may be assigned to **A** and/or **C**. We have observed through ^{1}H NMR monitoring of these resonances that the conversion of **B** to **3-Os** (in the hydrolysis of **2-Os**) was more favorable in DCM; the conversion did not occur in

THF/H_2O even after 72 h but upon removal of the solvents and re-dissolution in DCM, the conversion was complete within 5 min. A similar observation was made for the conversion of **C** to **5-Os** and **6-Os** (in the hydrolysis of **1-Os**). These observations are consistent with the more favorable elimination of NaCl (as depicted in the proposed pathways) in DCM than in THF/H_2O, which helps drive the conversion towards completion.

It has been pointed out that the chemical shifts of the metal hydride resonances may not be a reliable guide to the nature of the hydrides (terminal vs bridging) [13,14]. We have attempted to verify our assignments of the resonances to terminal metal hydrides through a GIAO calculation; the calculated terminal hydride resonances for **A**-**C** ranged from -6.28 to -8.32, in fairly good agreement with the experimental values (see supplementary data Table S2). We have also attempted to optimize alternative structures of these intermediates with bridging hydride ligands but were unsuccessful; the final optimized structures all adopted terminal hydrides.

The two competitive pathways **I** and **II** for the hydrolysis of **1-Os** also account for the lower reaction rate and higher yield observed in the hydrolysis of **2-Os**; the lower yield of **3-Os** from **1-Os** via pathway **II** may be accounted for by the attack of OH^- on the $SbPh_2Cl$ ligand in **1-Os**, leading to other side-products. Our computational study using density functional theory gives the Gibbs' free energies for steps **III** and **IV** to be about -72 and -40 KJ/mol, respectively. Unlike **A** and **B**, the two likely isomers for **C** have a significantly large difference in energy; the value given here is for the reaction to the more stable isomer. This suggests that pathway **III** is thermodynamically more favorable than **IV**, and may account for the higher yield of **3-Os** compared to that of **5-Os** and/or **6-**

Os. Attempts at increasing the yields of **5-Os** and/or **6-Os** through the use of different bases (NaOH or KOH) were unsuccessful.

Our attempt at preparing a ruthenium analogue to **5-Os** through a similar procedure was unsuccessful because the synthesis of $Ru_3(CO)_{11}(SbPh_2Cl)$, **1-Ru**, via the reaction of $Ru_3(CO)_{11}(NCCH_3)$ with $SbPh_2Cl$ in various solvents (DCM, THF or CH_3CN) failed; decomposition was rapid even at 0 °C, with only small amounts of $Ru_3(CO)_{12}$, **7-Ru**, being recovered. Radical-initiated substitution in **7-Ru** with benzophenone ketyl had been shown to be stoichiometrically specific and occurred under mild conditions [15]. Our attempt at the substitution of **7-Ru** with $SbPh_2Cl$ using catalytic amount of the ketyl radical failed, however, presumably due to destruction of the ketyl radical by the $SbPh_2Cl$. Surprisingly, treatment of **7-Ru** with a stoichiometric amount of the ketyl radical followed by the addition of excess $SbPh_2Cl$ afforded the ruthenium analogue of **5-Os**, *viz*. $Ru_6(CO)_{20}(\mu\text{-}SbPh_2)_2$, **5-Ru**, in moderate yield (Scheme 3). The reaction time for the first step had to be kept short (~15 min) in order to avoid the over-reduction of **7-Ru** to divalent anionic species [16], and the second step was essentially instantaneous; prolonged stirring led to a reduced yield. An attempt at extending this methodology for the synthesis of **5-Os** failed, probably due to the lower reactivity of $Os_3(CO)_{12}$ towards the ketyl radical.

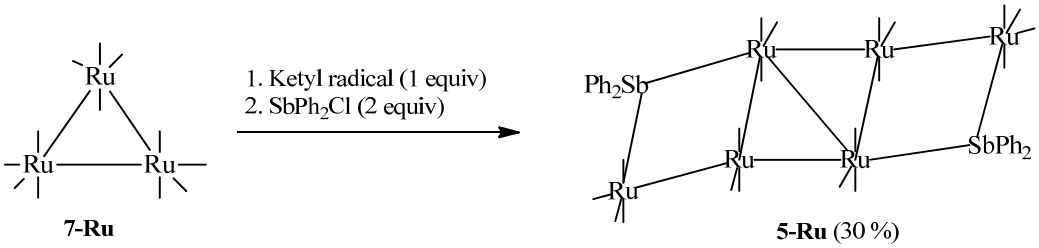

7-Ru **5-Ru** (30 %)

Scheme 3. Reaction of **7-Ru** with $SbPh_2Cl$ in the presence of ketyl radical.

Cluster **5-Ru** is not stable in coordinating solvents such as methanol and THF, but is relatively stable in DCM under ambient conditions; there were no signs of decomposition over several days. It has been fully characterized, including by single-crystal X-ray diffraction studies on two different crystals, with one being a solvate. The ORTEP plot from the non-solvate, depicting its molecular structure, is shown in Fig. 2.

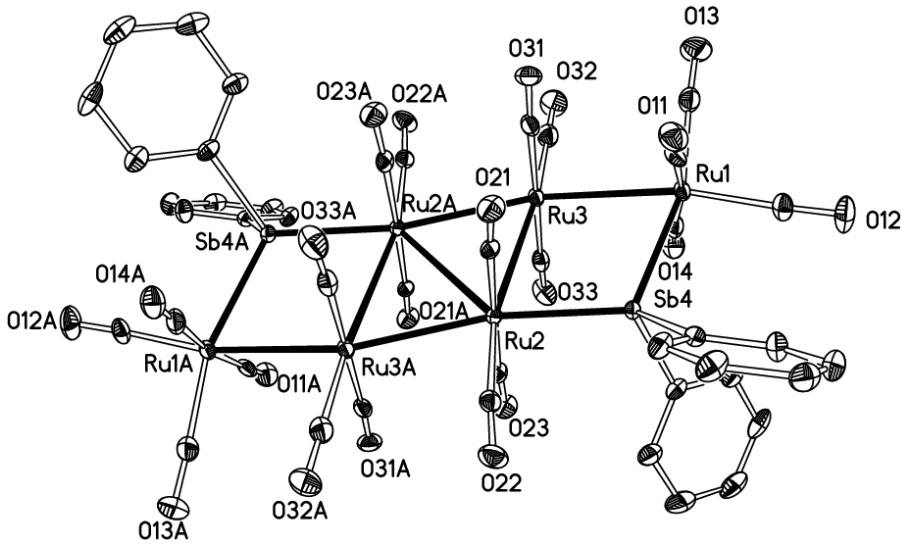

Fig. 2. ORTEP plot of the molecular structure of **5-Ru** with thermal ellipsoids at the 50% probability level. Organic hydrogen atoms have been omitted for clarity.

It is known that **7-Ru** can be reduced to $[Ru_6(CO)_{18}]^{2-}$ or $[Ru_3(CO)_{11}]^{2-}$ with one or two equivalents of the ketyl radical, respectively [16,17], and it has been suggested that $[Ru_6(CO)_{18}]^{2-}$ came from the further reaction of $[Ru_3(CO)_{11}]^{2-}$ with **7-Ru**, although there has been little mechanistic information on this. The possibility that **5-Ru** was formed from an Ru_6 carbonyl species, possibly a precursor to $[Ru_6(CO)_{18}]^{2-}$, was ruled out as the reaction of $[Ru_3(CO)_{11}]^{2-}$ (prepared in accordance with the literature method) with one equivalent of **7-Ru** (to form the higher nuclearity, anionic cluster *in situ*), followed by $SbPh_2Cl$, afforded no identifiable product.

We believe that radical-initiated substitution in **7-Ru** did occur according to the pathway established by Bruce (Scheme 4) [15b], i.e., an initial single electron transfer to **7-Ru** to form the radical anion **E** followed by a ligand addition to **F**. In the case of triorganophosphanes, -arsanes and –stibanes, that is followed by loss of a CO and electron-transfer, resulting in overall radical-catalysed ligand substitution. In our case, however, a stoichiometric amount of the ketyl radical was required and was added to **7-Ru** prior to the addition of $SbPh_2Cl$. This indicated that the ketyl radical acted as a reducing agent rather than as a catalyst. From **F**, the reaction probably proceeded via chloride elimination and formation of an Ru-Sb bond to the 17-electron intermediate **G**, which then dimerised to **5-Ru** through a decarbonylation. Attempts at trapping one or more of the radical intermediates with TEMPO afforded unidentified mixtures.

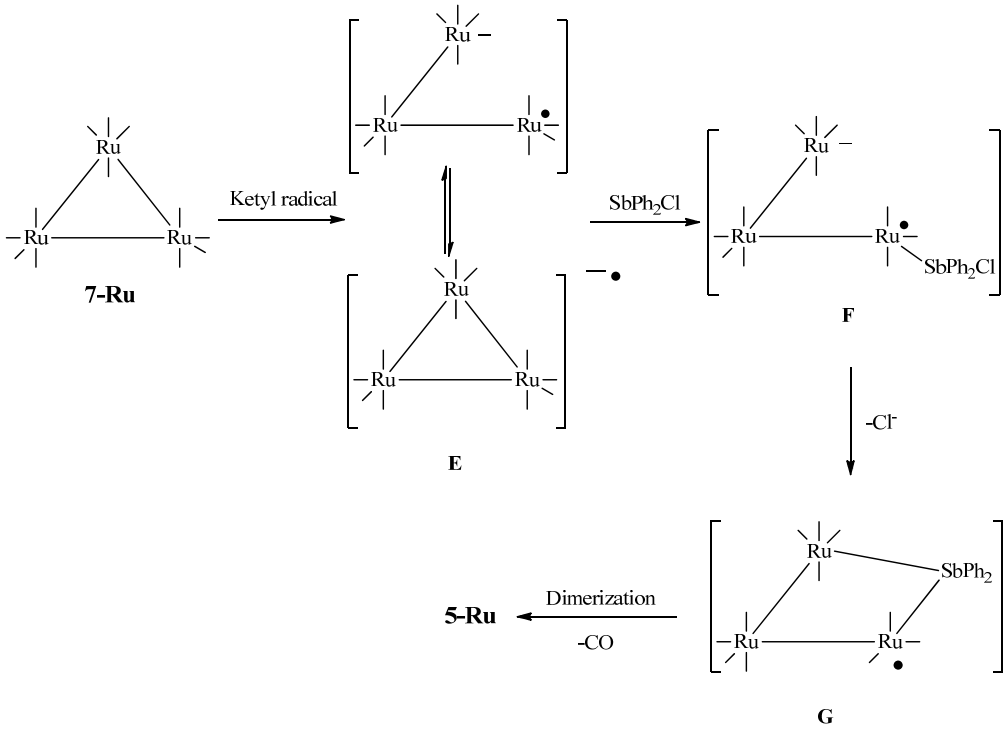

Scheme 4. Proposed formation pathway to **5-Ru**.

The electronic spectrum (DCM solution) of **5-Os** exhibited two absorption bands at 488 nm and 572 nm, while that for **5-Ru** were at 565 nm and 678 nm (see supplementary data Fig. S11), suggesting that **5-Ru** has a smaller HOMO-LUMO gap, and may thus be more readily attacked by nucleophiles. Experimentally, both reacted with two-electron donors to afford substituted derivatives (Scheme 5). The reaction with t-butylisonitrile was significantly faster, and only the mono-substituted derivative was isolated; attempts at obtaining more highly substituted products afforded a complex mixture. Both mono- and di-substituted derivatives were obtained for the phosphanes, and these did not undergo further substitution.

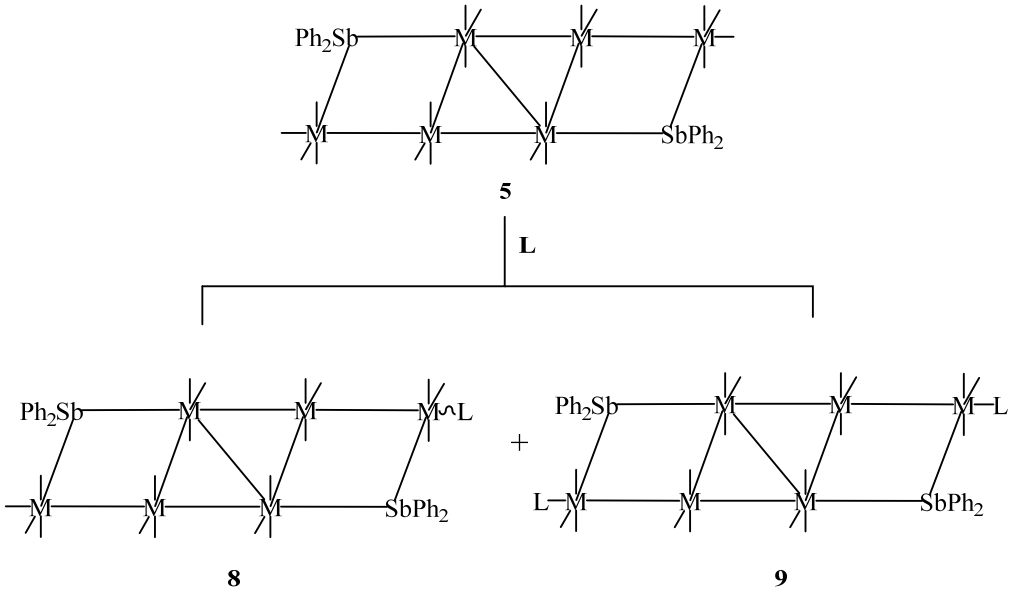

L = PMe_3 (a)	8%	72%
PPh_3 (b)	46%	40%
^{t}BuNC (c)	52%	-

Scheme 5. Reaction of clusters **5** with two-electron donors.

The monosubstituted derivatives **8** are soluble in most organic solvents but are unstable in coordinating solvents, while the disubstituted derivatives **9** are poorly soluble.

The molecular structures of **8b-Ru**, **9a-Os**, **9b-Ru** and **8c-Ru** have been characterized by single-crystal diffraction studies, although the data quality for the latter two were poor but sufficient to allow unambiguous determination of the heavy atom positions; the ligand positions are less clear. The ORTEP plots depicting the molecular structures of **8b-Ru** and **9a-Os** are given in Fig. 3 and Fig. 4, respectively.

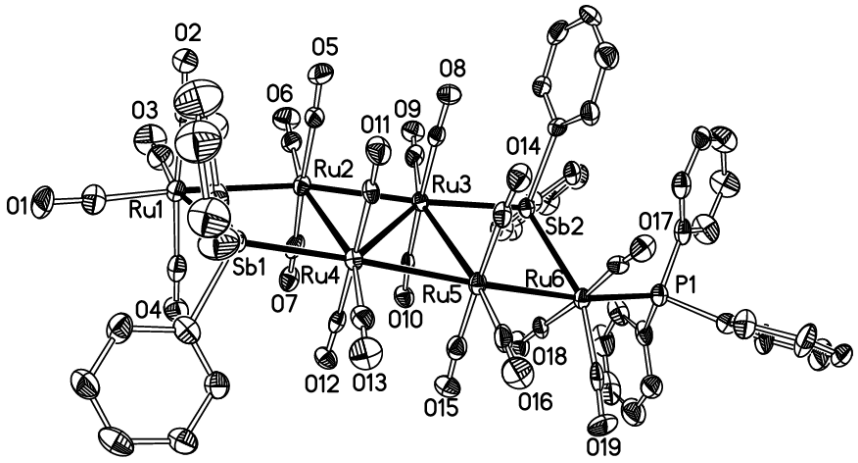

Fig. 3. ORTEP plot of the molecular structure of **8b-Ru**. Thermal ellipsoids are drawn at the 50% probability level. Organic hydrogen atoms have been omitted for clarity.

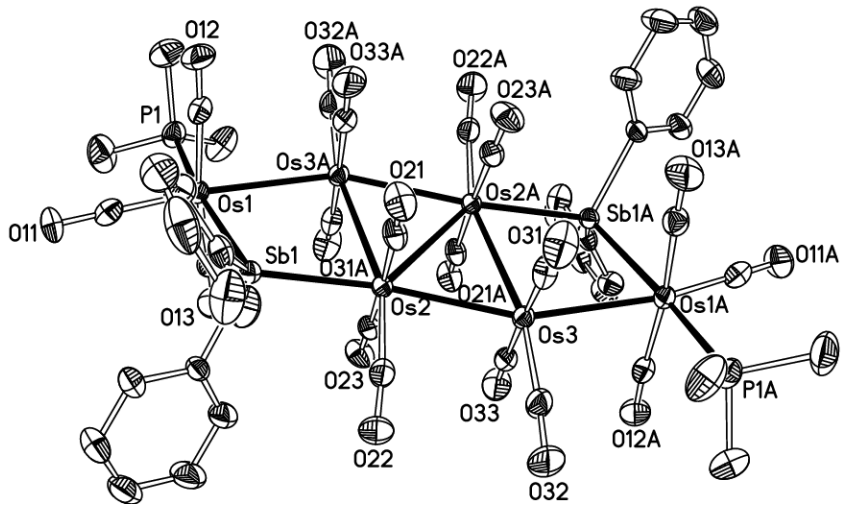

Fig. 4. ORTEP plot of the molecular structure of **9a-Os**. Thermal ellipsoids are drawn at the 30% probability level. Organic hydrogen atoms have been omitted for clarity.

Substitution appears to favour an "outer" ruthenium atom, i.e., the "spike" atom with respect to the transition metal framework. As expected on the basis of homometallic osmium and ruthenium cluster chemistry, the phosphanes tend to occupy equatorial positions while ^{t}BuNC occupies the axial position [18]. While the PPh_3 ligands in **8b-Ru** and **9b-Ru** occupy equatorial positions *cis* to the adjacent antimony, the two PMe_3 ligands in **9a-Os** adopt *trans* configurations with respect to their corresponding adjacent antimony atoms; it is unclear why this is so. The electronic spectra of these derivatives show that the main absorption maxima of **8a-Os** and **9a-Os** (585 nm and 598 nm, respectively) are red-shifted with respect to that for **5-Os** (see supplementary data Fig. S11). This is also the case with **5-Ru**; the main absorption maxima of **8b-Ru** and **9b-Ru** are red-shifted to 570 nm and 575 nm, respectively. These red shifts presumably point to a decrease in the HOMO-LUMO gap with stronger electron-donors in equatorial positions.

Crystallographic discussion

Selected bond parameters for **5-Os** and **5-Ru**, and their substituted derivatives **8b-Ru** and **9a-Os**, are collected in Table 1. There are two independent molecules in the asymmetric unit of **5-Os**, with each molecule located at an inversion centre. For **5-Ru**, a THF solvate (**5-Ru·THF**) was also obtained. All the clusters have a valence electron count of 94, which is consistent with the seven Os-Os or Ru-Ru bonds observed. The M_6Sb_2 cluster cores are all fairly planar; the maximum deviation from the metal plane in **5-Os** was < 0.05 Å, slightly larger (0.15 to 0.18 Å) in **5-Ru**, and slightly larger still upon substitution (0.14 Å and 0.32 Å for **9a-Os** and **8b-Ru**, respectively). As mentioned earlier, the several homometallic Ru carbonyl clusters with two-dimensional metal cores which

have been reported prior to this work either exhibited large deviations from planarity [19], or were supported by ancillary ligands on one side of that (quasi-)plane [19a,b,h]. The Ru_6Sb_2 clusters here represent the first truly raft-like clusters of ruthenium not structurally supported by ancillary ligands.

The central M_4 tetrametallic unit tend to be associated with the shortest (M2-M3 and M5-M6) and the longest (M2-M6 and M3-M5) metal-metal bond lengths. As has already been pointed out, group 15 ligand substitution tends to lengthen the M-M bond *cis* to it [15d,20]. Among the M-Sb bonds, those *trans* to an M-M bond are shorter than those *trans* to a CO or PR_3. We had earlier advocated considering the metal-carbonyl bond in terms of the sum of the M-C and C-O bond lengths rather than either of the individual bond parameters [10]. As expected, the metal-carbonyl bond lengths associated with equatorial CO ligands are shorter than those for the axial CO ligands, with a clear gap (> 0.01 Å) between their ranges. The exception are for the equatorial CO ligands *trans* to an Sb atom (M-CO(trans)), which tend to lie within the range for the axial carbonyls, indicating that the $SbPh_2$ group has a strong *trans* influence.

Table 1. Common atom-labeling scheme and selected bond lengths (Å) and angles (deg) for **5-Os**, **5-Ru**, **8b-Ru** and **9a-Os**.

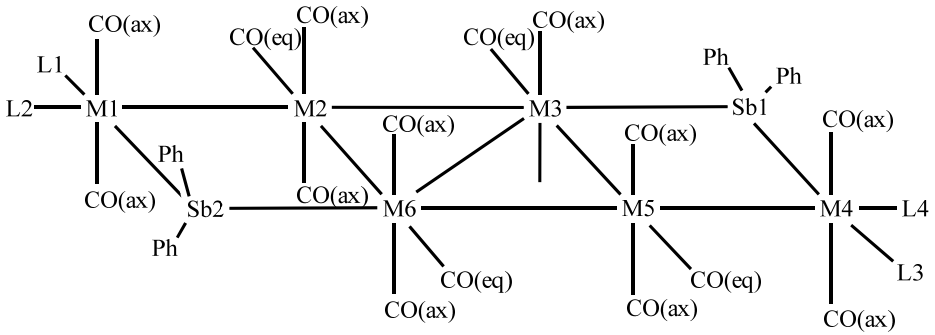

	5-Os	**5-Ru**	**5-Ru·THF**	**8b-Ru**	**9a-Os**
	M = Os; L1 = L2 = L3 = L4 = CO	M = Ru; L1 = L2 = L3 = L4 = CO		M = Ru; L1 = L2 = L3 = CO; L4 = PPh_3;	M = Os; L1 = L3 = PMe_3; L2 = L4 = CO
	Molecule 1; Molecule 2				
M1-M2	2.9295(5); 2.9293(4)	2.9080(5)	2.9274(5)	2.939(6)	2.9564(5)
M2-M3	2.8736(5); 2.9293(4)	2.8730(5)	2.8938(5)	2.860(5)	2.8885(5)
M2-M6	2.9325(4); 2.9364(4)	2.9230(5)	2.9166(5)	2.922(6)	2.9420(5)
M3-M6	2.8903(7); 2.9142(6)	2.9352(7)	2.8767(5)	2.909(6)	2.9085(6)
M3-M5	2.9325(4); 2.9364(4)	2.9230(5)	2.9594(5)	2.920(6)	2.9420(5)
M4-M5	2.9295(5); 2.9293(4)	2.9080(5)	2.9097(5)	2.914(5)	2.9564(5)
M5-M6	2.8736(5); 2.9293(4)	2.8730(5)	2.8476(5)	2.852(5)	2.8885(5)

M1-Sb2	2.6579(7); 2.6594(6)	2.6507(5)	2.6396(5)	2.663(6)	2.6452(6)
M3-Sb1	2.6225(7); 2.6272(6)	2.6168(5)	2.6124(5)	2.642(5)	2.6302(5)
M4-Sb1	2.6579(7); 2.6594(6)	2.6507(5)	2.6579(5)	2.655(5)	2.6452(6)
M6-Sb2	2.6225(7); 2.6272(6)	2.6168(5)	2.5976(5)	2.612(5)	2.6302(5)
M-CO(ax)[a]	3.074-3.099; 3.073-3.093	3.070-3.091	3.074-3.095	3.057-3.105	3.068-3.085
M-CO(eq)[a]	3.019-3.044; 3.024-3.057	3.011-3.059	3.011-3.069	3.004-3.042	3.013-3.038
M-CO(trans)[a,b]	3.083; 3.088	3.097	3.090, 3.095	3.082	-
M-P	-	-	-	2.373(13)	2.392(2)
Mean (maximum) deviation of metal core (Å)	0.036 (0.040); 0.049 (0.050)	0.149 (0.154)	0.166 (0.185)	0.225 (0.322)	0.137 (0.156)

[a] Sum of M-C and C-O bond lengths.

[b] Equatorial CO trans to Sb.

Concluding remarks

In this study, we reported the synthesis and characterization of two higher nuclearity, raft-like, M_6Sb_2 (M = Ru or Os) clusters. These were obtained via two very different synthetic routes, and reaction pathways leading to their formation were proposed. These raft-like clusters readily underwent ligand substitution with two-electron donors, exemplified by PPh_3, PMe_3 and ^{t}BuNC. Remarkably, ligand substitution did not appear to induce any significant distortion in the structures.

Experimental Section

General Data. All manipulations were carried out in an argon atmosphere with standard Schlenk techniques. Reagent grade solvents were dried by the standard procedures and were freshly distilled prior to use. The ketyl radical (*ca*. 0.025 M) was prepared according to the literature mothod [15b]. Compounds $SbPh_2Cl$ [21], and $Os_3(CO)_{11}(NCCH_3)$ [22], were prepared as described in the literature. TLC separations were carried out on 20 x 20 cm^2 plates coated with silica gel 60 F254, from Merck. NMR spectra were recorded on a JEOL ECA-400 MHz NMR spectrometer. ^1H and $^{13}C\{^1H\}$ chemical shifts were referenced to the residual resonances of the respective deuterated solvents; $^{31}P\{^1H\}$ chemical shifts were referenced to external 85% aqueous H_3PO4. Mass spectra were recorded in electrospray ionization (ESI) mode on a Waters Q-Tof Premier mass spectrometer. Elemental analyses were carried out in-house. Electronic spectra were recorded on a Perkin Elmer Lambda 900 spectrometer as DCM solutions.

Preparation of 5-Os: $Os_3(CO)_{11}(NCCH_3)$ (40 mg, 43 μmol) was dissolved in dry THF (14 ml) followed by the addition of $SbPh_2Cl$ (14 mg, 45 μmol). The resulting yellow mixture was stirred at room temperature for 12 h; the IR spectrum showed the formation

of **1-Os** and depletion of $Os_3(CO)_{11}(NCCH_3)$. To the reaction mixture, Na_2CO_3 (30-50 mesh, 4.7 mg, 44 μmol) and deionized water (0.70 ml) were added and stirred at room temperature for another 6 h, leading to an orange solution. The solvents were then removed in *vacuo* to give a bluish yellow residue. Redissolution in dry DCM (10 ml) and stirring for another 0.5 h afforded a bluish yellow solution. Removal of the solvent followed by separation of the residue by TLC, with DCM/hexane (1:1, v/v) as the eluent, gave several bands.

Band 1, yellow, was identified as $Os_3(CO)_{10}(\mu\text{-H})(\mu\text{-SbPh}_2)$, **3-Os**. R_f = 0.70. Yield = 14 mg (28%).

Band 2, light yellow, was identified as $Os_3(CO)_{10}(\mu\text{-SbPh}_2)_2$, **4-Os**. R_f = 0.55. Yield = 2.0 mg (7.0%).

Band 3, green, was **6-Os** the identity of which has not been established. R_f = 0.45. Yield = 2.5 mg. IR (CH_2Cl_2): ν(CO) 2117w, 2101s, 2060sh, 2037s, 2017w, 1990w, 1969w cm^{-1}; ^1H NMR (C_6D_6) δ 7.76 (d, 4H, PhH), 7.69 (d, 4H, PhH), 6.90-7.05 (dd, 12H, PhH) ppm. ESI-MS^+ (*m/z*): 2254 $[M+H]^+$, 2177 $[M+H\text{-Ph}]^+$, 2149 $[M+H\text{-CO-Ph}]^+$.

Band 4, purple, was identified as $Os_6(CO)_{20}(\mu\text{-SbPh}_2)_2$, **5-Os**. R_f = 0.40. Yield = 2.5 mg (5.0%). IR (CH_2Cl_2): ν(CO) 2118w, 2105s, 2038s, 2014w, 1993m, 1971w cm^{-1}. ^1H NMR (CD_2Cl_2) δ 7.50 (dd, 8H, PhH), 7.39-7.44 (m, 12H, PhH) ppm; ^1H NMR (C_6D_6) δ 7.60 (dd, 8H, PhH), 6.87-6.97 (m, 12H, PhH) ppm. $^{13}C\{^1H\}$ NMR (CD_2Cl_2): δ (CO) 197.12 (2C), 185.02 (2C), 184.61 (1C), 179.63 (1C), 173.44 (2C), 172.65 (1C), 166.07 (1C), δ (Ph) 134.70, 130.33, 129.18, 125.82 ppm. Anal. Calcd for $C_{44}H_{20}O_{20}Os_6Sb_2$: C 23.45, H 0.89. Found: C 23.51, H 0.60. ESI-MS^+ (*m/z*): 2254 $[M+H]^+$, 2149 $[M+H\text{-CO-Ph}]^+$.

Band 5, very light yellow, was identified as $Os_3(CO)_{11}(Cl)(\mu\text{-}SbPh_2)$, **2-Os**. R_f = 0.30. Yield = 1.0 mg (2.0%).

Reaction of 5-Os with PMe_3: Cluster **5-Os** (12 mg, 5.3 μmol) and PMe_3 (1.5 mg, 20 μmol) were dissolved in dry DCM (10 ml) and the mixture maintained at 0 °C. A solution of TMNO in dry CH_3CN (0.80 ml, 10.6 μmol) was added dropwise. The resulting light purple solution turned a darker blue after stirring for 6h, after which the solution was allowed to warm up to room temperature and stirred for another 72h. The solvents were then removed by rotary evaporator and the residue separated on silica TLC with DCM/Hexane (3:2, v/v) as eluent, giving two separable bands.

Band 1, blue, afforded **8a-Os** as the minor product. R_f = 0.65. Yield = 1.0 mg (8.2%). IR (CH_2Cl_2): ν(CO) 2111m, 2077s, 2044sh, 2033sh, 2027vs, 2002s, 1981w, 1975w, 1965w cm^{-1}. ^1H NMR (MeOD): δ 7.45-7.50 (m, 8H, Ph), 7.31-7.43 (m, 12H, Ph), 1.34 (s, 9H, CH_3) ppm; $^{31}P\{^1H\}$ NMR (C_6D_6) δ -60.98 (s) ppm. ESI-MS^+ (*m/z*): 2303 $[M+H]^+$.

Band 2, greenish blue, afforded **9a-Os** as the major product. R_f = 0.50. Yield = 9.0 mg (72%). IR (CH_2Cl_2): ν(CO) 2056m, 2021w, 2005vs, 1975w, 1965w, 1923w cm^{-1}. ^1H NMR (CD_2Cl_2): δ 7.69-7.71 (m, 8H, Ph), 7.54-7.56 (m, 12H, Ph), 1.33 (s, 18H, CH_3) ppm; $^{31}P\{^1H\}$ NMR (C_6D_6) δ -33.68 (s) ppm. Anal. Calcd for $C_{48}H_{38}O_{18}P_2Os_6Sb_2$: C 24.54, H 1.63. Found: C 24.54, H 1.20. ESI-MS^+ (*m/z*): 2350 $[M+H]^+$.

Preparation of 5-Ru: The cluster $Ru_3(CO)_{12}$, **7-Ru** (40 mg, 62 μmol) was dissolved in dry THF (8 ml). To this was added the ketyl radical (0.025 M, 2.5 ml, 62 μmol). The resulting mixture was stirred at room temperature for 15 min during which the color gradually changed from orange to dark red. Then $SbPh_2Cl$ (40 mg, 0.13 mmol) was added and the color immediately changed to blue-purple. The reaction mixture was

stirred for another 2 min. After removing the solvent, the residue was separated by TLC, with DCM/hexane (1:2, v/v) as the eluent, to give two main bands.

Band 1 was identified as unreacted $Ru_3(CO)_{12}$ (R_f = 0.75; yield = 3 mg).

Band 2, blue, was identified as $Ru_6(CO)_{20}(\mu\text{-}SbPh_2)_2$, **5-Ru**. R_f = 0.45. Yield = 16 mg (30% based on consumed $Ru_3(CO)_{12}$). IR (CH_2Cl_2): ν(CO) 2112w, 2096s, 2050sh, 2037s, 2016w, 1995m, 1975m cm^{-1}. ^1H NMR (C_6D_6): δ 7.69 (dd, 8H, PhH), 6.90-7.00 (m, 12H, PhH) ppm; ^1H NMR (CD_2Cl_2): δ 7.58 (dd, 8H, PhH), 7.41-7.44 (m, 12H, PhH) ppm; $^{13}C\{^1H\}$ NMR (CD_2Cl_2): δ (CO) 217.56 (2C), 213.72 (2C), 199.62 (1C), 197.79 (1C), 194.99 (2C), 193.16 (1C), 189.88 (1C), δ (Ph) 134.89, 131.62, 129.86, 129.18 ppm. Anal. Calcd for $C_{44}H_{20}O_{20}Ru_6Sb_2$: C 30.75, H 1.17. Found: C 31.30, H 1.38. ESI-MS^+ (*m/z*): 1719 $[M+H]^+$.

Reaction of 5-Ru with PPh_3: Cluster **5-Ru** (20 mg, 12 μmol) and PPh_3 (15 mg, 57 μmol) were dissolved in dry DCM (10 ml). The resulting blue-purple solution was stirred at room temperature for 48 h. The solution was then concentrated (to about 5 ml) whereupon **9b-Ru** precipitated out as a greenish-blue crystalline powder, which was separated by centrifugation, washed thrice with DCM/hexane (1:1, v/v), and air-dried. Yield = 10 mg (40% based on consumed **5-Ru**). IR (CH_2Cl_2): ν(CO) 2061s, 2040w, 2022s, 2007vs, 1962w cm^{-1}. ^1H NMR (C_6D_6) δ 7.71 (dd, 20H, PhH), 7.12 (t, 10H, PhH), 7.03 (m, 20H, PhH) ppm. $^{31}P\{^1H\}$ NMR (C_6D_6) δ -33.68 (s) ppm. Anal. Calcd for $C_{78}H_{50}O_{18}P_2Ru_6Sb_2$: C 42.83, H 2.30. Found: C 42.93, H 1.99. ESI-MS^+ (*m/z*): 2350 $[M+H]^+$.

The supernatant was separated by TLC, with DCM/hexane (1:2, v/v) as the eluent, to give two three bands.

Bands 1 and 3 were identified as unreacted **5-Ru** (1 mg) and a trace amount of **9b-Ru**, respectively.

Band 2, blue, afforded **8b-Ru** as the major product. Yield = 10 mg (46% based on consumed **5-Ru**). IR (CH_2Cl_2): ν(CO) 2103m, 2075s, 2048w, 2029vs, 2006s, 1979w, 1969w cm^{-1}. ^1H NMR (CD_2Cl_2) δ 7.56 (br, s, 5H, PhH), 7.38 (br, s, 10H, PhH), 7.08-7.27 (m, 20H, PhH) ppm. $^{13}C\{^1H\}$ NMR (CD_2Cl_2): δ (CO) 219.59 (2C), 218.62 (2C), 215.45 (2C), 213.89 (2C), 200.88 (1C), 200.16 (1C), 199.97 (2C, $^2J_{P-C}$ = 8Hz), 199.44 (1C, $^2J_{P-C}$ = 5Hz), 199.22 (1C), 198.22 (1C), 195.48 (2C), 194.20 (1C), 190.65 (1C), δ (Ph) 135.43, 134.93, 134.62, 134.16, 132.78, 132.67, 131.98, 130.75, 129.59, 129.17, 129.00, 128.76, 128.67 ppm. $^{31}P\{^1H\}$ NMR (CD_2Cl_2) δ 32.49 (s) ppm. Anal. Calcd for $C_{61}H_{35}O_{19}PRu_6Sb_2$: C 37.52, H 1.81. Found: C 37.01, H 1.58. ESI-MS^+ (*m/z*): 2350 $[M+H]^+$.

Reaction of 5-Ru with ^{t}BuNC: To a solution of **5-Ru** (20 mg, 12 μmol) in dry DCM (10 ml) was added a solution of ^{t}BuNC in dry hexane (0.20 ml, 12 μmol), dropwise. The resulting blue-purple solution was stirred at room temperature for 24h before solvent removal and separation of the residue on a silica column, with DCM/Hexane (1:1, v/v) as eluent, to afford two main bands.

Band 1, blue-purple, was identified as unreacted **5-Ru** (5 mg).

Band 2, blue-purple, afforded **8c-Ru** as the major product. R_f = 0.60. Yield = 8.0 mg (52% based on consumed **5-Ru**). IR (CH_2Cl_2): ν(*NC*) 2193w, 2173w; ν(CO) 2103m, 2073s, 2031vs, 2008w, 1991w, 1966w cm^{-1}. ^1H NMR (CD_2Cl_2) δ 7.66 (dd, 2H, PhH), 7.5-7.58 (m, 6H, PhH), 7.33-7.40 (m, 12H, PhH), 1.11 (s, 9H, ^{t}Bu) ppm. $^{13}C\{^1H\}$ NMR (CD_2Cl_2): δ (CO) 218.83 (1C), 218.55 (1C), 218.24 (1C), 218.17 (1C), 215.53 (1C), 214.57 (1C), 213.97 (1C), 213.58 (1C), 201.11 (1C), 200.71 (1C), 199.84 (1C), 198.41 (1C), 196.96

(1C), 195.62(1C), 195.57 (1C), 195.29 (1C), 194.14 (1C), 191.97 (1C), 190.50 (1C), δ (Ph) 135.51, 135.09, 134.95, 134.89, 134.81, 133.50, 132.66, 132.17, 131.28, 129.70, 129.51, 129.39, 129.23, 129.06, 128.96, 128.88, 29.99 ($C(CH_3)_3$), 29.22 ($C(CH_3)_3$) ppm. The ^{13}C resonance for the CN^tBu ligand was not observed, probably due to its accidental overlap with signals of CO ligands or its low intensity probably caused by its fluxionality or a process of dynamic loss and reattachment to Ru. $^{31}P\{^1H\}$ NMR (CD_2Cl_2) δ 32.49 (s) ppm. Anal. Calcd for $C_{48}H_{29}O_{19}NRu_6Sb_2$: C 32.50, H 1.65, N 0.79. Found: C 32.32, H 1.36, N 0.74. ESI-MS^+ (*m/z*): 2350 $[M+H]^+$.

Crystallographic analyses. Diffraction-quality crystals were obtained by slow evaporation of solutions of the clusters as follows: **5-Os** (dark red) from methanol/dichloromethane, **5-Ru** (dark blue-purple), **8b-Ru** (blue crystals) and **8c-Ru** (blue crystals) from dichloromethane/hexane, **5-Ru·THF** from THF/hexane, **9a-Os** (green) and **9b-Ru** (dark blue) from DCM. For clusters **5-Ru**, **5-Ru·THF** and **8b-Ru**, the X-ray diffraction intensity data were collected on a Bruker Kappa diffractometer equipped with a CCD detector, employing Mo Kα radiation (λ = 0.71073 Å), with the SMART suite of programs [23]; all the data were processed and corrected for Lorentz and polarization effects with SAINT and for absorption effects with SADABS [24]. For the others, intensity data was collected on a SuperNova (Dual source) Agilent diffractometer using either Mo Kα (λ = 0.71073 Å) (**5-Os**) or Cu Kα radiation (λ = 1.54184 Å) (**9a-Os**, **9b-Ru** and **8c-Ru**); the data was processed and corrected for absorption effects with CrysAlisPro [25]. All the structural solutions and refinements were carried out with the SHELXTL suite of programs [26]. All non-hydrogen atoms were refined with anisotropic

thermal parameters. Crystal data, data collection parameters, and refinement data are summarized in Table S1 (see supplementary data).

Computational studies. DFT calculations were performed with the Gaussian 09 suite of programs [27], utilizing B3LYP density-functional, together with an "ultrafine" numerical integration grid. The LanL2DZ (Los Alamos effective core potential double-z) basis set, together with d- or f-type polarization functions [28], was employed for the Os and Sb atoms while the 6-311G(2d, p) basis set was used for the remaining atoms. Spin-restricted calculations were used for geometry optimization. Harmonic frequencies were then calculated to characterize the stationary points as equilibrium structures with all real frequencies, and to evaluate zero-point energy (ZPE) corrections. Isotropic nuclear magnetic shielding constants were calculated using the gauge-including-atomic-orbital (GIAO) method at the HF level of theory with the same basis sets above, in a solvated phase (THF) using the PCM model [29]; chemical shifts δ were obtained as $\delta = \sigma_{ref} - \sigma_{orb}$, in which σ_{ref} is the shielding in TMS.

Supplementary material: Crystallographic data (excluding structure factors) for the structures in this paper have been deposited with the Cambridge Crystallographic Data Centre as supplementary publication numbers CCDC 1400549-53. Copies of the data can be obtained, free of charge, on application to CCDC, 12 Union Road, Cambridge CB2 1EZ, UK, (fax: +44 1223 336033 or e-mail: deposit@ccdc.cam.ac.uk). Spectroscopic and other data for all compounds, details of computed structures, and ORTEP plots of **8c-Ru** and **9b-Ru**.

Acknowledgement

This work was supported by Nanyang Technological University and the Ministry of Education (Research Grant No. M4011158). Y.-Z. Li thanks the university for a Research Scholarship. We also acknowledge Dr. Yan-Li Zhao for the use of his X-ray diffractometer and Dr. Pei-Zhou Li for assistance with the data collection on clusters **5-Os**, **9a-Os**, **9b-Ru** and **8c-Ru**.

Dedication: This article is dedicated to the late Lord Lewis of Newnham.

References

[1] (a) Clusters in Ligand Shells. In Clusters and Colloids, Wiley-VCH Verlag GmbH: 2007; pp 89-177; (b) F. Yang, E. Trufan, R. D. Adams, D. W. Goodman, J. Phys. Chem. C, 112 (2008) 14233–14235; (c) R. D. Adams, Q. Zhang, X. Yang, J. Am. Chem. Soc. 133 (2011) 15950-15953.

[2] (a) L. Pizzagalli, D. Stoeffler, F. Gautier, Phys. Rev. B 54 (1996) 12216–12224; (b) O. Waldmann, Coord. Chem. Rev. 249 (2005) 2550–2566.

[3] (a) R. J. Goudsmit, B. F. G. Johnson, J. Lewis, P. R. Raithby, K. H. Whitmire, J. Chem. Soc., Chem. Commun. (1982) 640-642; (b) R. J. Goudsmit, B. F. G. Johnson, J. Lewis, P. R. Raithby, K. H. Whitmire, J. Chem. Soc., Chem. Commun. (1983) 246-247; (c) R. J. Goudsmit, J. G. Jeffrey, B. F. G. Johnson, J. Lewis, R. C. S. McQueen, A. J. Sanders, J.-C. Liu, J. Chem. Soc., Chem. Commun. (1986) 24-26; (d) J. G. Jeffrey, B. F. G. Johnson, J. Lewis, P. R. Raithby, D. A. Welch, J. Chem. Soc., Chem. Commun. (1986) 318-320; (e) M. P. Diebold, S. R. Drake, B. F. G. Johnson, J. Lewis, M. McPartlin, H. Powell, J. Chem. Soc., Chem. Commun. (1988) 1358-1360; (f) K. Sze-Yin Leung, W.-T. Wong, J. Chem. Soc., Dalton Trans. (1999) 2521-2524.

[4] (a) R. D. Adams, B. Captain, W. Fu, M. D. Smith, J. Am. Chem. Soc. 124 (2002) 5628-5629; (b) R. D. Adams, B. Captain, W. Fu, M. B. Hall, J. Manson, M. D. Smith, C. E. Webster, J. Am. Chem. Soc. 126 (2004) 5253-5267; (c) R. D. Adams, B. Captain, L. Zhu, Inorg. Chem. 45 (2005) 430-436; (d) Y. Liu, R. Ganguly, H. V. Huynh, W. K. Leong, Organometallics 32 (2013) 7559-7563.

[5] J. A. Cabeza, P. García-Álvarez, D. Polo, Inorg. Chem. 50 (2011) 6195-6199.

[6] (a) R. D. Adams, B. Captain, L. Zhu, Organomettalics 25 (2006) 2049; (b) R. D. Adams, B. Captain, M. B. Hall, E. Trufan, X. Yang, J. Am. Chem. Soc. 129 (2007) 12328-12340; (c) R. D. Adams, B. Captain, E. Trufan, J. Cluster Sci. 18 (2007) 642−659; (d) R. D. Adams, B. Captain, E. Trufan, J. Organomet. Chem. 693 (2008) 3593-3602; (e) R. D. Adams, Y. Kan, Q. Zhang, Organometallics 31 (2012) 8639-8646.

[7] W. K. Leong, F. W. B. Einstein, R. K. Pomeroy, Organometallics 15 (1996) 1589-1596.

[8] (a) J. Howard, S. A. R. Knox, F. G. A. Stone, P. Woodward, J. Chem. Soc. D: Chem. Commun. (1970) 1477-1478; (b) J. Howard, P. Woodward, J. Chem. Soc. A: Inorg. Phys. Theor. (1971) 3648-3650.

[9] (a) W. K. Leong, G. Chen, Organometallics 20 (2001) 2280-2287; (b) K. H. Chan, W. K. Leong, K. H. G. Mak, Organometallics 25 (2006) 250-259; (c) Y.-Z. Li, R. Ganguly, W. K. Leong, Organometallics 33 (2014) 823-828.

[10] Y.-Z. Li, R. Ganguly, W. K. Leong, Organometallics 33 (2014) 3867-3876.

[11] W. K. Leong, G. Chen, J. Chem. Soc., Dalton Trans. (2000) 4442-4445.

[12] Cluster **2-Os** (24 mg, 20 μmol) was dissolved in dry THF (10 ml) followed by addition of Na_2CO_3 (3.6 mg, 34 μmol) and deionized H_2O (0.5 ml), the resulting mixture was stirred at room temperature for 78h, monitored by IR spectra. The solvents were removed and the residue redissolved in DCM for 5 min. Then the residue was separated on silica TLC with DCM/Hexane (1:1, v/v) as eluent to give **3-Os** as the sole separable product (Yield = 17.5 mg, 75%).

[13] M. A. M. Al-Ibadi, S. B. Duckett, J. E. McGrady, Dalton Trans. 41 (2012) 4618–4625.

[14] We wish to thank one of the reviewers for alerting us to this work.

[15] (a) M. L. Bruce, D. C. Kehoe, J. G. Matisons, B. K. Nicholson, P. H. Rieger, M. L. Williams, J. Chem. Soc., Chem. Commun. (1982) 442-444; (b) M. I. Bruce, J. G. Matisons, B. K. Nicholson, J. Organomet. Chem. 247 (1983) 321-343; (c) M. I. Bruce, Coordin. Chem. Rev. 76 (1987) 1-43; (d) M. I. Bruce, M. J. Liddell, C. A. Hughes, B. W. Skelton, A. H. White, J. Organomet. Chem. 347 (1988) 157-180; (e) M. I. Bruce, B. K. Nicholson, M. L. Williams, T. Arliguie, G. Lavigne, Inorg. Synth. (2007) 221-230.

[16] (a) C. M. T. Hayward, J. R. Shapley, Inorg. Chem. 21 (1982) 3816-3820; (b) J. F. Corrigan, M. Dinardo, S. Doherty, G. Hogarth, Y. Sun, N. J. Taylor, A. J. Carty, Organometallics 13 (1994) 3572-3580.

[17] (a) C. C. Nagel, J. C. Bricker, D. G. Alway, S. G. Shore, J. Organomet. Chem. 219 (1981) C9-C12; (b) A. A. Bhattacharyya, C. C. Nagel, S. G. Shore, Organometallics 2 (1983) 1187-1193.

[18] G. Chen, W. K. Leong, J. Organomet. Chem. 574 (1999) 276-278.

[19] (a) U. Bodensieck, H. Stoeckli-Evans, G. Süss-Fink, Angew. Chem. Int. Edit. 30 (1991) 1126-1127; (b) S. Jeannin, Y. Jeannin, F. Robert, C. Rosenberger, Inorg. Chem. 33 (1994) 243-252; (c) B. R. Cockerton, A. J. Deeming, Polyhedron 13 (1994) 2085-2088; (d) K. K. H. Lee, W. T. Wong, J. Organomet. Chem. 503 (1995) C43-C45; (e) L. A. Hoferkamp, G. Rheinwald, H. Stoeckli-Evans, G. Süss-Fink, Organometallics 15 (1996) 1122-1127; (f) J. A. Cabeza, I. del Río, V. Riera, F. Grepioni, Organometallics 16 (1997) 812-815; (g) C. Sze-Wai Lau, W.-T. Wong, J. Chem. Soc., Dalton Trans. (1998) 3391-3396; (h) S. Du, B. E. Hodson, P. Lei, T. D. McGrath, F. G. A. Stone, Inorg. Chem. 46 (2007) 6613-6620.

[20] (a) W. K. Leong, Y. Liu, J. Organomet. Chem. 584 (1999) 174-178; (b) S. S. Sirat, I. A. Khan, O. B. Shawkataly, M. M. Rosli, Z. Anorg. Allg. Chem. 640 (2014) 2019-2024.

[21] M. Nunn, D. B. Sowerby, D. M. Wesolek, J. Organomet. Chem. 251 (1983) C45-C46.

[22] (a) B. F. G. Johnson, J. Lewis, D. A. Pippard, J. Chem. Soc., Dalton Trans. (1981) 407-412; (b) J. N. Nicholls, M. D. Vargas, A. J. Deeming, S. E. Kabir, Inorg. Synth. 28 (1990) 232-235.

[23] SMART version 5.628; Bruker AXS Inc.: Madison, WI, USA, 2001.

[24] Sheldrick, G. M., SADABS, 1996.

[25] Agilent Technologies, CrysAlisPro, Version 1.171.35.21b.

[26] SHELXTL version 5.1; Bruker AXS Inc.: Madison, WI, USA, 1997.

[27] Gaussian 09, Revision D.01, M. J. Frisch, G. W. Trucks, H. B. Schlegel, G. E. Scuseria, M. A. Robb, J. R. Cheeseman, G. Scalmani, V. Barone, B. Mennucci, G. A.

Petersson, H. Nakatsuji, M. Caricato, X. Li, H. P. Hratchian, A. F. Izmaylov, J. Bloino, G. Zheng, J. L. Sonnenberg, M. Hada, M. Ehara, K. Toyota, R. Fukuda, J. Hasegawa, M. Ishida, T. Nakajima, Y. Honda, O. Kitao, H. Nakai, T. Vreven, J. A. Montgomery Jr., J. E. Peralta, F. Ogliaro, M. Bearpark, J. J. Heyd, E. Brothers, K. N. Kudin, V. N. Staroverov, R. Kobayashi, J. Normand, K. Raghavachari, A. Rendell, J. C. Burant, S. S. Iyengar, J. Tomasi, M. Cossi, N. Rega, N. J. Millam, M. Klene, J. E. Knox, J. B. Cross, V. Bakken, C. Adamo, J. Jaramillo, R. Gomperts, R. E. Stratmann, O. Yazyev, A. J. Austin, R. Cammi, C. Pomelli, J. W. Ochterski, R. L. Martin, K. Morokuma, V. G. Zakrzewski, G. A. Voth, P. Salvador, J. J. Dannenberg, S. Dapprich, A. D. Daniels, Ö. Farkas, J. B. Foresman, J. V. Ortiz, J. Cioslowski, D. J. Fox, Gaussian, Inc., Wallingford CT, 2009.

[28] (a) Gaussian Basis Sets for Molecular Calculations, Huzinaga, S.; Andzelm, J., Elsevier: Amsterdam; 1984, p. 23; (b) A. W. Ehlers, M. Böhme, S. Dapprich, A. Gobbi, A. Höllwarth, V. Jonas, K. F. Köhler, R. Stegmann, A. Veldkamp, G. Frenking, Chem. Phys. Lett. 208 (1993) 111-114.

[29] (a) R. Ditchfield, Mol. Phys. 27 (1974) 789-807; (b) J. R. Cheeseman, G. W. Trucks, T. A. Keith, M. J. Frisch, J. Chem. Phys. 104 (1996) 5497-5509.